

1 **Synthetic Metabolic Pathway for the Production of 1-Alkenes from Lignin-derived**
2 **Molecules**

3 Jin Luo*, Tapio Lehtinen, Elena Efimova, Ville Santala, and Suvi Santala

4 Department of Chemistry and Bioengineering, Tampere University of Technology, 33720,
5 Tampere, Finland

6 *corresponding author

7 E-mail address: jin.luo@tut.fi

8 **Abstract**

9 Integration of synthetic metabolic pathways to catabolically diverse chassis provides new
10 opportunities for sustainable production. One attractive scenario is the use of abundant
11 waste material to produce readily collectable product, minimizing production costs.
12 Towards that end, we established the production of semivolatile medium-chain α -olefins
13 from lignin-derived monomers: we constructed 1-undecene synthesis pathway in
14 *Acinetobacter baylyi* ADP1 using ferulate as the sole carbon source. In order to overcome
15 the toxicity of ferulate, we first applied adaptive laboratory evolution, resulting in a highly
16 ferulate-tolerant strain. Next, we demonstrated the 1-undecene production from glucose by
17 heterologously expressing a fatty acid decarboxylase UndA and a thioesterase ‘TesA in the
18 wild type strain. Finally, we constructed the alkene synthesis pathway in the ferulate-
19 tolerant strain. We were able to produce 1-undecene from ferulate and collect the product
20 from the culture headspace without downstream processing. This study demonstrates the
21 potential of bacterial lignin upgradation into value-added products.

22 **Keywords:** lignin; ferulate, 1-alkenes; adaptive laboratory evolution; *Acinetobacter baylyi*

23 **1 Introduction**

24 The concerns of energy security and environmental issues are driving the development of
25 sustainable and environment-friendly processes for the production of chemicals and fuels.
26 To that end, lignocellulose biorefining has gained substantial attention as a solution to
27 mitigate the dependence on petroleum-based industry (Ragauskas, 2006). Lignocellulose is
28 the most abundant biopolymer on Earth, holding a huge potential as the feedstock for
29 sustainable bioproduction. However, efficient use of lignocellulose is somewhat hindered
30 as lignin, a major component of lignocellulose, is poorly utilized due to its recalcitrance and
31 inherent heterogeneity. Along with the development of second generation biorefineries, an
32 increasing amount of lignin will be generated as a by-product (Ragauskas et al., 2014). In
33 addition, pulp and paper industry produce large quantities of lignin-rich waste as a by-
34 product (Ragauskas et al., 2014; Rinaldi et al., 2016). Thus, it is of high priority to develop
35 technologies for lignin valorization with respect to economic efficiency and environmental
36 sustainability.

37 To boost the value of lignin, strategies have been developed for lignin depolymerization
38 and subsequent valorization (Abdelaziz et al., 2016). Lignin depolymerization yields
39 various aromatic molecules (monomers, oligomers and polymers), which complicates the
40 downstream processing. Nevertheless, it has been reported that some organisms can utilize
41 these lignin-derived molecules (LDMs) as carbon sources and convert them into central
42 intermediates, protocatechuate and catechol (Abdelaziz et al., 2016; Harwood and Parales,
43 1996; Linger et al., 2014). The central intermediates will be further converted to acetyl-

44 CoA and succinyl-CoA through β -ketoacid pathway and enter the citric acid cycle.

45 *Acinetobacter baylyi* ADP1 is one of the microorganisms that has been reported to

46 catabolize various LDMs and even directly depolymerize lignin (Gerischer, 2008; Salmela

47 et al., 2018; Salvachúa et al., 2015). Moreover, *A. baylyi* ADP1 is readily genetically

48 engineered due to its natural transformability and recombination ability (Metzgar et al.,

49 2004), and have been shown to produce a variety of industrially relevant compounds by

50 native and non-native pathways (Lehtinen et al., 2018, 2017, Santala et al., 2014a, 2011).

51 Thus, *A. baylyi* ADP1 could be a potential candidate for lignin valorization.

52 LDMs are known to be toxic to microorganisms (Cerisy et al., 2017; Ibraheem and Ndimba,

53 2013; Mills et al., 2009), which also hinders the use of LDMs as substrates. In order to

54 develop a tolerant strain, adaptive laboratory evolution (ALE) can be employed. In ALE,

55 microorganisms are successively cultivated under rationally designed selection pressure,

56 e.g. elevated concentration of inhibitors (Dragosits and Mattanovich, 2013). The approach

57 can lead to the strains with beneficial changes allowing them to adapt to the stressful

58 condition. ALE has been successfully applied on various microorganisms to improve their

59 tolerance against inhibitory compounds (Almario et al., 2013; Atsumi et al., 2010; Cerisy et

60 al., 2017).

61 Bio-based production of hydrocarbons, such as alkanes and alkenes, is of great interest due

62 to their use as advanced “drop-in” biofuels and various fine chemicals (Choi and Lee, 2013;

63 Lee et al., 2018; Sarria et al., 2017; Zhou et al., 2018). In nature, some organisms have been

64 found to possess the pathways for the synthesis of medium-chain (C8-C12) or long-chain

65 (>C12) hydrocarbons (Sarria et al., 2017; Schirmer et al., 2010). Particularly, medium-

66 chain α -olefins, such as 1-undecene, are attractive molecules for their broad use in
67 detergents, plasticizers and monomers for elastomers (Sarria et al., 2017). In addition, the
68 molecules can accumulate extracellularly and are semivolatile, which allow them to be
69 collected directly from the culture vessel without cell harvesting and/or product extraction,
70 significantly reducing the costs and labour of downstream processing. Recently, a single
71 gene *undA* originated from *Pseudomonas* has been discovered to be responsible for 1-
72 undecene (C11) biosynthesis (Rui et al., 2014). UndA is an oxygen-activating, nonheme
73 iron (II)-dependent decarboxylase that converts free fatty acids (FFAs) to the corresponding
74 terminal alkenes. The enzyme accepts fatty acids with chain length from 10 to 14 as
75 substrates. The gene has been heterologously expressed e.g. in *E. coli* for 1-undecene
76 production (Rui et al., 2014). Other possible alkene synthesis pathways include polyketide
77 synthase (PKS) pathway and head-to-head hydrocarbon synthesis pathway, in which
78 multiple enzymes and reactions are involved (Beller et al., 2010; Liu et al., 2015). In
79 comparison, the one-step decarboxylation of FFAs catalyzed by UndA is simpler and has a
80 narrower substrate spectrum (Kang and Nielsen, 2017).

81 In this study, we employed *A. baylyi* ADP1 for the production of 1-undecene from a lignin
82 derived model compound, ferulate. We applied ALE to improve the tolerance of *A. baylyi*
83 ADP1 against ferulate, and established a synthetic pathway for the direct conversion of
84 LDMs to 1-undecene (Figure 1). We demonstrate the potential of catabolically diverse
85 bacteria for the synthesis of industrially relevant compounds from an abundant and
86 sustainable substrate.

87 **2 Results**

88 **2.1 Adaptation of *A. baylyi* ADP1 to high concentration of ferulate**

89

90 In order to improve the growth of *A. baylyi* ADP1 on the lignin-derived compounds, we
91 carried out ALE using ferulate as the model compound. Ferulic acid is an important
92 building block during lignin biosynthesis (Zhao and Moghadasian, 2008). Its salt form,
93 ferulate, is one of the major lignin-derived aromatic molecules that can be obtained from
94 alkaline pretreated lignin (De Menezes et al., 2017; Vardon et al., 2015). Wild type ADP1
95 was cultivated in mineral salts medium supplemented with 45 mM ferulate as a sole energy
96 and carbon source, after which the cells were sequentially transferred to fresh medium
97 before reaching a stationary phase. The concentration of ferulate was gradually increased to
98 125 mM by the end of the evolution, which was the highest concentration introduced. After
99 the evolution, isolates from two concurrently evolved populations were compared. The
100 isolates from population 1 showed better and more consistent growth in ferulate than those
101 from population 2. The best performing isolate, designated as adapted ADP1, was selected
102 for further comparison with wild type ADP1. In adapted ADP1, colony morphology did not
103 change based on the observation on plates. In addition, the natural transformability was
104 maintained after the ALE.

105 **2.2 Comparison of growth in ferulate between wild type and adapted ADP1**

106 To compare the growth between wild type and adapted ADP1 in ferulate, both strains were
107 precultivated in mineral salts medium supplemented with 15 mM ferulate, after which cells
108 were transferred to fresh mediums supplemented with different concentrations of ferulate.

109 Generally, adapted ADP1 showed higher tolerance towards ferulate. As ferulate
110 concentration was increased, the growth rates of both strains were reduced (Figure 2A and
111 B), but the degree of reduction for adapted ADP1 was much smaller than that of the wild
112 type. Wild type ADP1 showed poor growth in 80 mM ferulate and the growth was
113 completely inhibited when ferulate concentration was 100 mM. In contrast, adapted ADP1
114 still exhibited prominent growth in 100 mM ferulate (Figure 2A). In 80 mM, adapted ADP1
115 also exhibited faster growth than wild type and reached higher optical density (OD) (Figure
116 S2).

117 In the aromatic catabolizing pathway of ADP1, ferulate is first converted into vanillate
118 (Fischer et al., 2008). Thus, the growth comparison was also performed using vanillate (15
119 mM, 45 mM, 75 mM and 100 mM) as a sole carbon source. Similarly, adapted ADP1
120 showed advantage over wild type in terms of growth on vanillate (Figure S3); Wild type
121 showed slightly slower growth and lower final OD than the adapted ADP1 already in 15
122 mM vanillate. As the concentration was increased, the growth of wild type ADP1 was
123 inhibited to a larger extent. In comparison, adapted ADP1 exhibited similar growth profile
124 as when grown on ferulate. Interestingly, adapted ADP1 did not show significantly
125 improved tolerance against *p*-coumarate, another LDM which can also be catabolized by
126 ADP1 via β -keto adipate pathway (data not shown).

127 **2.3 Constructing the synthesis pathway for 1-undecene production**

128 To confer 1-undecene production, we heterologously expressed *undA* and '*tesA* in *A. baylyi*
129 ADP1. The thioesterase '*TesA* (a leaderless version of *TesA* that is targeted in cytosol), is
130 responsible for the conversion of acyl-ACP to fatty acid, the precursor for alkene synthesis,

131 and therefore hypothesized to benefit the synthesis (Steen et al., 2010). For the expression,
132 a cyclohexanone-inducible promoter ChnR/*P_{chnB}* originally isolated from *A. johnsonii* was
133 used (Steigedal and Valla, 2008). The expression system has been previously characterized
134 in *E. coli* and *P. putida* (Benedetti et al., 2016). For testing the functionality of the
135 expression system in *A. baylyi*, a plasmid pBAV1C-chn-GFP was constructed. Induction
136 factor of 52 was obtained for 1 mM cyclohexanone after 3 hours of induction, indicating
137 strong expression and high signal/noise ratio.

138 Plasmid pBAV1C-chn was constructed and used as the vector for the expression of *undA*
139 and '*tesA*. Three different plasmids were constructed: pBAV1C-chn-*undA*, pBAV1C-chn-
140 '*tesA*, and pBAV1C-chn-'*tesA-undA* (Figure S1). *A. baylyi* ADP1 was then transformed
141 with pBAV1C-chn (empty plasmid control) and the three expression plasmids, designated
142 as ADP1-empty plasmid, ADP1 *UndA*, ADP1 '*tesA*, and ADP1 '*tesA-undA*.

143 To select the optimal construct, we compared the production of 1-undecene between the
144 transformants containing different plasmids. The transformants were cultivated in MA/9
145 medium supplemented with 5% glucose, 0.2% casein amino acid, and 25 µg/ml
146 chloramphenicol. The cells were induced with 1 mM cyclohexanone when the OD reached
147 1. After 1 h of induction, the cells were transferred to sealed vials and cultivated overnight.
148 The produced and evaporated alkenes were directly analyzed from the headspace of the
149 culture vials by solid phase micro-extraction (SPME)–gas chromatography mass
150 spectrometry (GCMS). The production of 1-undecene by different strains is shown in
151 Figure 3. ADP1-empty plasmid produced only traces of 1-undecene (4.46 ± 0.07 µg/L).
152 The production was greatly increased by expressing *undA* alone in ADP1 (418 ± 24 µg/L)

153 while expressing *tesA* alone did not have a great influence on the production (5.06 ± 0.33
154 $\mu\text{g/L}$). ADP1 *tesA-undA* had the highest production ($694 \pm 76\mu\text{g/L}$), which was 1.7 fold
155 higher than with ADP1 *undA*. In addition, signal of 1-tridecene were detected in the
156 cultivation with ADP1 *tesA-undA* (Figure S5). At the end of the cultivation, ADP1 with
157 empty plasmid and ADP1 *undA* reached the OD of more than 2 while the other strains had
158 the OD approximately 1.5 (Figure S4). Based on the results, pBAV1C-chn-*tesA-undA* was
159 selected for 1-undecene production from ferulate.

160 **2.4 1-Undecene production from ferulate with adapted ADP1**

161 We demonstrated that the highest 1-undecene production was obtained with pBAV1C-chn-
162 *tesA-undA* among the constructed plasmids. Thus, adapted ADP1 was transformed with
163 the construct and designated as adapted ADP1 *tesA-undA*. Both adapted ADP1 *tesA-undA*
164 and ADP1 *tesA-undA* were precultivated in mineral salts medium supplemented with 5
165 mM ferulate, followed by batch cultivations in 110 mM ferulate. During the cultivation,
166 biomass and ferulate concentration were monitored. The detection of 1-undecene was
167 carried out by SPME-GCMS.

168 As expected, adapted ADP1 *tesA-undA* showed distinct advantage over ADP1 *tesA-undA*
169 when cultivated in approximately 110 mM ferulate (Figure 4 A). ADP1 *tesA-undA* showed
170 almost no growth or ferulate consumption during the cultivation, the final OD being 0.21.
171 On the contrary, adapted ADP1 *tesA-undA* showed efficient growth in approximately 110
172 mM ferulate; the OD was 3.6 at the time of induction, and 5.5 after the following 4.5 h of
173 incubation with the inducer. At this time-point, 52 mM ferulate was left in the culture.
174 During the cultivation in sealed vials, due to the oxygen limitation, the OD did not change

175 greatly and only a small amount of additional ferulate was consumed. At the end of
176 cultivation, 72 ± 7.5 $\mu\text{g/L}$ 1-undecene was detected from the cultivation of adapted ADP1
177 '*tesA-undA* while no 1-undecene was produced by ADP1 '*tesA-undA* (Figure 4 B).

178 **3 Discussion**

179 Lignin has a great potential as a sustainable substrate for bio-based production of fuels and
180 chemicals: It has high energy and carbon content, it is renewable and widely available, and
181 large quantities of lignin-rich waste streams are generated by e.g. bioethanol and paper
182 industry. The practical problem with its utilization is that the typically employed production
183 hosts cannot degrade and further metabolize the aromatic compounds that are the
184 constituents of lignin (Beckham et al., 2016). Furthermore, the aromatic compounds are
185 strong growth inhibitors (Mills et al., 2009). In this study, we established a novel bacterial
186 production platform that utilizes a major constituent of lignin, ferulate, as the sole carbon
187 source. *A. baylyi* ADP1 was employed as the host due to its ability of aromatic compound
188 utilization, adaptability, and the possibility to funnel the intermediates to products of
189 interest.

190 Although *A. baylyi* ADP1 can utilize ferulate as a sole carbon source, it was found out that
191 the growth rate is reduced or completely inhibited at concentrations relevant for a
192 bioprocess. The mechanism of the inhibition caused by ferulate has not been characterized
193 in detail, but a general mechanism of the inhibition caused by phenolic compounds is
194 thought to be related to their hydrophobicity (Fitzgerald et al., 2004; Mills et al., 2009);
195 phenolic compounds can target cell membranes and interact with lipids and membrane-
196 embedded proteins, breaking the integrity of the membranes. In order to allow the use of

197 LDMs as a substrate for both cell growth and product synthesis, it is a prerequisite to
198 overcome the toxicity of these compounds to host cells. To this end, ALE was employed
199 for *A. baylyi* ADP1 to improve the tolerance and growth on ferulate. As a result of ALE, the
200 growth inhibition caused by ferulate was significantly reduced. The adapted strain showed
201 not only robust growth in high ferulate concentration (up to 125 mM) while the growth of
202 wild type was completely inhibited, but also more prominent growth than wild type in low
203 ferulate concentration. In a previous study, the genes involved in the tolerance towards
204 coumaric acid, another lignin-derived phenolic compound, were identified in *Pseudomonas*
205 *putida* (Calero et al., 2018). Most of the identified genes were related to membrane stability,
206 transport system, and membrane proteins while the genes involved in the degradation of the
207 compounds only play minor roles in the tolerance (Calero et al., 2018). Those identified
208 genes seem to be more related to global stress handling. In this study, it seems that the
209 improved tolerance is resulted from a different mechanism, since the adapted strain shows
210 improved tolerance specific to ferulate and vanillate but not to coumarate. The additional
211 methoxyl group on the benzene ring of ferulate and vanillate may play an important role in
212 the mechanism. The correlations between the improved phenotype and the genotype remain
213 to be investigated in future.

214 Alkenes represent industrially relevant platform chemicals used in a broad range of
215 applications and products. Interestingly, the short and medium chain molecules are
216 semivolatile, potentially allowing straight-forward collection and continuous production
217 processes. As a proof-of-concept, our aim was to demonstrate the production of 1-undecene
218 from ferulate without downstream processing. To confer the pathway for alkene production,

219 three different plasmids were constructed to express either *undA*, *'tesA*, or both *undA* and
220 *'tesA* in the wild type ADP1. Free fatty acids with chain lengths from 10 to 14 typically
221 serve as the substrate for *UndA*, whereas acyl-CoA and acyl-ACPs are unlikely converted
222 to alkenes (Rui et al., 2014). However, the strain possessing only *undA* produced 418 ± 24
223 $\mu\text{g/L}$ 1-undecene (93-fold more than the control strain) from glucose, indicating the
224 existence of available FFAs in ADP1 for 1-undecene synthesis. It has been reported that *A.*
225 *baylyi* possesses a natural intracellular thioesterase, which can produce FFAs ranging from
226 C6 to C18 from acyl-ACP (Zheng et al., 2012), potentially explaining why *UndA* alone can
227 confer alkene production in ADP1. The trace amounts of 1-undecene detected in the control
228 strain indicates the existence of natural alkene synthesis mechanism in ADP1. The
229 expression of *'tesA* can further convert acyl-ACPs to FFAs, which provides more
230 precursors for 1-undecene synthesis. Although *'Tesa* prefers C14 acyl-ACPs as the
231 substrate, it also accepts C12 acyl-ACP, the precursor for 1-undecene synthesis (Choi and
232 Lee, 2013). Hence, it was expectable that ADP1 *'tesA-undA* produced the most 1-undecene,
233 $694 \pm 76\mu\text{g/L}$, improving the production by 1.7 fold in comparison with ADP1 *undA* alone.
234 Since it was demonstrated that the co-expression of *undA* and *'tesA* improved the
235 production of 1-undecene in the ADP1 wild type, the same construct pBAV1C-*chn-'tesA-*
236 *undA* was transformed to the adapted ADP1 to produce 1-undecene from ferulate. After the
237 transformation, the adapted strain still maintained excellent growth in high ferulate
238 concentration. 1-Undecene with a concentration of $72 \pm 7.5 \mu\text{g/L}$ was successfully
239 produced, when ferulate was used as the only carbon source. The biomass and ferulate

240 concentration did not significantly change during the cultivation in sealed vials, which is
241 probably due to the limitation of oxygen.

242 In a previous study, Chen et al. (2015) expressed the one-step decarboxylase OleT in *S.*
243 *cerevisiae* and increased the production of total intracellular alkenes 67.4-fold to 3.7 mg/L
244 by combinatorial metabolic engineering strategies and process optimization. Liu et al.
245 (2014) expressed OleT in FFAs overproducing *E. coli* and obtained 97.6 mg/L of total
246 intra- and extracellular alkenes, the highest reported production so far. The availability of
247 FFAs plays an important role in alkene production. However, in the aforementioned studies,
248 most alkenes produced had chain lengths of 15 and 17, only small amount of 1-undecene
249 (C11) was produced. Compared to OleT, UndA has a narrower substrate spectrum (C10 to
250 C14). Rui et al. (2014) overexpressed an UndA homolog in *E. coli* and obtained 6 mg/L
251 extracellular 1-undecene production without strain optimization. UndB was later found to
252 be the most efficient among UndA and OleT for 1-undecene production (Rui et al., 2015).
253 Co-expression of Pmen_4370, an UndB homolog, and UcFatB2, a C12-specific
254 thioesterase for lauric acid (C12) synthesis, conferred extracellular 1-undecene production
255 of a titer of ~55 mg/L in *E. coli* (Rui et al., 2015). Thus, the alkene chain length can be
256 controlled by the specificity of the key enzymes towards the substrates.

257 Compared to the previous studies, the 1-alkene titers obtained here were low, 694 ± 76
258 $\mu\text{g/L}$ from glucose and $72 \pm 7.5 \mu\text{g/L}$ from ferulate. However, it should be noted that in the
259 latter case, all the required energy and carbon for both generating the catalyst (biomass) and
260 the production of 1-undecene was obtained from ferulate, emphasizing the potential of the
261 used cell platform. In addition, as the goal was to demonstrate the direct production and

262 collection of 1-undecene without downstream processing, only the alkenes that were
263 secreted by the cells were analyzed. In order to improve the production, the culture set-up
264 should be further developed and optimized; in the current system, the cell growth and
265 consequently 1-undecene production rapidly cease due to the oxygen limitation in sealed
266 vials. For example, cultivations in a bioreactor enabling continuous culture and product
267 recovery would likely significantly improve the productivity. In addition, employing
268 molecular level strategies, such as increasing the availability of FFAs and co-factors,
269 selection of more efficient enzymes specific to medium-chain length substrate, and
270 blocking of competing pathways could further improve the production (Chen et al., 2015;
271 Kang and Nielsen, 2017; Peralta-Yahya et al., 2012).

272 As demonstrated in this study medium-chain alkenes can be produced directly from ferulate
273 through microbial conversion. However, to realize the upgrading of lignin to medium-chain
274 alkenes, many factors should be considered. For example, efficient substrate conversion is
275 the key factor for high productivity. Technologies for lignin depolymerization, such as
276 alkaline pretreatment of lignocellulose, yields low molecular weight LDMs which can serve
277 as the substrates for microbial conversion (Abdelaziz et al., 2016). However, considering
278 that the depolymerization of lignin gives rise to a highly heterogeneous mixture of different
279 acids and phenolic compounds, it is necessary to evaluate the utilization of mixed LDMs
280 and even real depolymerization products. It has been reported that the catabolism of
281 aromatic compounds via β -ketoacid pathway is affected by different regulatory
282 mechanisms (Bleichrodt et al., 2010; Fischer et al., 2008). In order to allow efficient
283 utilization of mixed substrates, further engineering should be employed to reduce the

284 carbon catabolite repression, e.g., by deletion of regulatory elements (Vardon et al., 2015).
285 In addition, improvement of the tolerance against mixed LDMs is also crucial for obtaining
286 high substrate conversion rate.

287 **4 Conclusions**

288 In this study, we aimed to demonstrate the potential of lignin-derived compounds as
289 substrates for the bioproduction of industrially relevant compounds. To that end, we
290 established the production of α -olefins (namely 1-undecene) by a synthetic pathway in *A.*
291 *baylyi* ADP1 using ferulate, a model compound for lignin monomer, as the sole carbon
292 source. The tolerance of *A. baylyi* ADP1 against ferulate was significantly improved by
293 ALE, which allowed the use of high ferulate concentration for the production. Our study
294 emphasizes the importance of host selection, and promotes the use of *A. baylyi* ADP1 as a
295 potential chassis for lignin valorization.

296 **5 Methods**

297 **5.1 Strains**

298 *E.coli* XL1-Blue (Stratagene, USA) was used for plasmid construction and amplification.
299 Wild type *A. baylyi* ADP1 (DSM 24193) was used as the parental strain in ALE to develop
300 adapted ADP1. Wild type *A. baylyi* ADP1 was transformed with plasmid pBAV1C-chn,
301 pBAV1C-chn-*undA*, pBAV1C-chn-*'tesA*, pBAV1C-chn-*undA-'tesA* and pBAV1C-chn-
302 *'tesA-undA*, designated as ADP1 empty plasmid, ADP1 *undA*, ADP1 *'tesA*, ADP1 *undA-*
303 *'tesA* and ADP1 *'tesA-undA*, respectively. ADP1 empty plasmid was used as control. The

304 adapted ADP1 was transformed with pBAV1C-*chn-tesA-undA* and designated as adapted
305 ADP1 *tesA-undA*.

306 5.2 Media

307 Luria-Bertani medium (10 g/L tryptone, 5 g/L yeast extract, 1 g/L NaCl) was used for
308 plasmid construction and transformation of wild type *A. baylyi*ADP1. The medium was
309 supplemented with 1% glucose as carbon source and 25 µg/ml chloramphenicol as
310 antibiotic when needed. For solid medium, 15 g/L agar was added.

311 Minimal salts medium (MA/9) was used for the cultivation of plasmid selection. The
312 composition was as follow: Na₂HPO₄ 4.40 g/L, KH₂PO₄ 3.40 g/L, NH₄Cl 1.00 g/L,
313 nitrilotriacetic acid 0.008 g/L, NaCl 1.00 g/L, MgSO₄ 240.70 mg/L, CaCl₂ 11.10 mg/L,
314 FeCl₃ 0.50 mg/L. The medium was supplemented with 0.2% casein amino acid, 5% glucose
315 and 25 µg/ml chloramphenicol when indicated.

316 Mineral salts medium as described by Hartmans et al. (1989) was used for the ALE
317 cultivation, the growth comparison in ferulate (wild type ADP1 vs. adapted ADP1), the
318 transformation of adapted ADP1 and the cultivation of 1-undecene production from ferulate.
319 This medium was applied in the experiments related to adapted ADP1 to maintain its
320 evolved properties, as the strain was adapted with the medium. The composition was shown
321 as follow: K₂HPO₄ 3.88 g/L, NaH₂PO₄ 1.63 g/L, (NH₄)₂SO₄ 2.00 g/L, MgCl₂.6H₂O 0.1 g/L,
322 Ethylenediaminetetraacetic acid (EDTA) 10 mg/L, ZnSO₄.7H₂O 2 mg/L, CaCl₂.2H₂O, 1
323 mg/L, FeSO₄.7H₂O 5 mg/L, Na₂MoO₄.2H₂O 0.2 mg/L, CuSO₄.5H₂O 0.2 mg/L,
324 CoCl₂.6H₂O 0.4 mg/L, MnCl₂.2H₂O 1 mg/L. This medium was supplemented with

325 different concentrations of ferulate (15-125mM for ALE, 15-100 mM for growth
326 comparison, 100 mM for the transformation of adapted ADP1 and 110 mM for 1-undecene
327 production). To prepare the stock solution (200 mM) of ferulate, proper amount of ferulic
328 acid (Sigma-Aldrich) was added to deionized water, after which equimolar amount of
329 NaOH was slowly added while stirring until ferulic acid was completely dissolved. For
330 solid medium, 15 g/L agar was added. Chloramphenicol (25 μ g/ml) was added when needed.

331 **5.3 Adaptive laboratory evolution**

332 The ferulate-tolerant strains were evolved by a short-term serial passage in mineral salts
333 medium supplemented with ferulate as sole carbon source. Wild type *A. baylyi* ADP1 was
334 first cultivated on solid mineral salts medium containing 15 mM ferulate. Single colony
335 was selected and precultivated in Erlenmeyer flask (100 ml) containing 10 ml medium
336 supplemented with 45 mM ferulate at 30 °C, 300 rpm. When reaching log phase, the cells
337 were cryopreserved as parental strain and the culture was passaged to two Erlenmeyer
338 flasks (100 ml) containing the same medium as in the precultivation. The two populations
339 were evolved in parallel. The concentration of ferulate was initially 45 mM and gradually
340 increased during the evolution to maintain the selection pressure. Cells were passaged to
341 fresh medium before entering into stationary phase to avoid unwanted mutation. Before
342 each passage, the OD of the culture was measured. The amount of inoculum was adjusted
343 daily to make the initial OD of each cultivation between 0.03 and 0.1. The cells were
344 cryopreserved at - 80 °C every two passages. The evolution went on for two months and 61
345 transfers were performed, corresponding to more than 350 generations. After the evolution,
346 single colonies from both populations were screened out on plates. The strain with the best

347 growth in ferulate, designated as adapted ADP1, was further compared with wild type
348 ADP1 (the parental strain).

349 **5.4 Comparison of growth in ferulate between wild type and adapted ADP1**

350 Wild type and adapted ADP1 were precultivated in 5 ml mineral salts medium
351 supplemented with 15 mM ferulate at 30 °C and 300 rpm. After 24 h, the cells from both
352 precultures were transferred to 96-well plate containing 200 µl mineral salts medium
353 supplemented with different concentrations of ferulate (15 mM, 30 mM, 45 mM, 60 mM,
354 80 mM and 100 mM) respectively. Each cultivation was performed in triplicate. The cells
355 were then incubated in Spark multimode microplate reader (Tecan, Switzerland) at 30 °C
356 for 72 h. Shaking was performed for 5 min twice an hour with a frequency of 54 rpm. The
357 optical density at 600 nm (OD600) was measured every hour.

358 Wild type and adapted ADP1 were also compared regarding the growth in vanillate, the
359 metabolite derived from ferulate in the aromatic catabolizing pathway. The same processes
360 as above were used for the comparison but vanillate was used instead of ferulate.

361 **5.5 Plasmid construction and transformation**

362 Plasmid construction was carried out using *E. coli* XL-1 Blue as host. The reagents for PCR,
363 digestion and ligation were provided by Thermo Scientific (USA) and used according to
364 provider's instruction. The primers used in this study are listed in table 1.

365 The plasmid pBAV1C-chnR/pChnB designated as pBAV1C-chn was constructed as
366 follows. First, the plasmid pBAV1C-T5-GFP, which was constructed by Santala et al.
367 (2014b), was amplified with the primers ab151 and ab152 to remove internal NdeI-site

368 from the plasmid backbone. The PCR product was self-ligated and transformed to *E. coli*
369 XL1-Blue strain. The obtained plasmid was named as pBAV1C-T5-GFP. Then, the
370 fragment containing the regulator *chnR* and its cognate promoter *pChnB* was amplified
371 from plasmid pSCM (a kind gift from Standard European Vector Architecture database
372 (Spain)) (Benedetti et al., 2016), using primers ab155 and ab156. To obtain pBAV1C-chn,
373 the amplified fragment was cloned to the pBAV1Cd plasmid backbone according to the
374 BioBrick assembly standard 10 using *EcoRI* and *PstI* sites.

375 For the initial characterization of cyclohexanone-inducible promoter system (*ChnR/P_{chnB}*)
376 in *A. baylyi* ADP1, a plasmid pBAV1C-chn-GFP was constructed as follows. The gene
377 fragment encoding monomeric and superfolder green fluorescent protein variant (GFP) was
378 PCR amplified from the pSCM plasmid using biobrick suffix and prefix primers, GFP fwd
379 and GFP rev. The fragment was BioBrick-cloned to pBAV1C-chn plasmid to obtain
380 pBAV1C-chn-GFP plasmid which was then transformed into *E. coli* XL-1 Blue. Verified
381 pBAV1C-chn-GFP construct was transformed into *A. baylyi* ADP1 by natural
382 transformation; Briefly, ADP1 was streaked on LA plate (containing 1% glucose). The cells
383 were incubated at 30°C overnight. On the second day, 0.5 µl of plasmid was dropped on the
384 top of a single colony and the cells were incubated for another day. On the third day, the
385 enlarged single colony were picked up and mixed with 50-100 µl LB medium. The mixture
386 was spread onto LA plate (containing 1% glucose and 25 µg/ml chloramphenicol) and
387 incubated at 30 °C until colonies appeared.

388 The gene *undA* was amplified with primer vs15_2 44 and vs15_1 68 using the genomic
389 DNA of *Pseudomonas putida* KT2440 as template. The fragment was cloned to pBAV1C-

390 chn with BioBrick assembly standard using restriction sites XbaI/SpeI and PstI. The
391 resulting construct was designated as pBAV1C-chn-*undA*. The gene '*tesA* was amplified
392 with tl15 and tl16 from the genome of *E. coli* MG1655 and cloned to pBAV1C-chn,
393 resulting in pBAV1C-chn-'*tesA*. The construct pBAV1C-chn-*undA* was further digested
394 with SpeI and PstI and ligated with the previously digested *undA*, resulting in the construct
395 pBAV1C-chn-'*tesA-undA*. The former two plasmids contain only *undA* or '*tesA*
396 respectively. The latter plasmid contains both '*tesA* and *undA*.

397 The transformation of *E. coli* was carried out using electroporation and the transformants
398 was screened on LA plates containing 25 µg/ml chloramphenicol. *A. baylyi* ADP1 was
399 transformed with the three constructed plasmids and the empty pBAV1C-chn. The adapted
400 ADP1 was transformed with pBAV1C-chn-'*tesA-undA*. The transformation was carried out
401 as described by Metzgar et al. (2004), with an exception that mineral salts medium
402 containing 100 mM ferulate was used as the medium for the transformation. The constructs
403 were verified by restriction analysis.

404 **5.6 Cultivation**

405 For testing the functionality of (*ChnR/P_{chnB}*), ADP1 carrying pBAV1C-chn-GFP plasmid
406 was cultivated in minimal salts medium containing 1% glucose, 0.2% casein amino acid
407 and 25 µg/ml chloramphenicol at 30 °C and 300 rpm. When the optical density at
408 wavelength 600 nm (OD600) reached 0.5-1, 1 mM cyclohexanone was added in the culture.
409 Cultivation without the addition of cyclohexanone was used as reference. The cultivation
410 was performed in duplicate. Samples were taken for OD600 and fluorescence after 3 hours
411 of cultivation. For fluorescence measurement, appropriate dilution was made to ensure that

412 samples contained the same amount of biomass. Fluorescence measurement was performed
413 with Spark multimode microplate reader (Tecan, Switzerland) with wavelengths 485 nm
414 (excitation) and 510 nm (emission) and the signal was proportioned to that of the non-
415 induced cells.

416 The cultivation for plasmid selection was carried out with the three constructed strains,
417 ADP1 *undA*, ADP1 *'tesA*, and ADP1 *'tesA-undA*. ADP1 containing empty plasmid was
418 used as control. Cultivation was performed in duplicate. Cells were precultivated in 5ml LB
419 medium containing 0.4% glucose and 25 µg/ml chloramphenicol. After overnight
420 cultivation, cells were transferred to 6 ml MA/9 medium containing 5% glucose, 0.2%
421 casein amino acid and 25 µg/ml chloramphenicol and cultivated at 30 °C and 300 rpm.
422 Initial OD was made to 0.05. Cells were induced with 1 mM cyclohexanone after 5 h of
423 cultivation (OD around 1). After 1 h of induction, 5 ml culture was transferred to sealed
424 headspace 20 ml vials (Agilent Technology, Germany) containing a stir bar and incubated
425 at 25 °C and 300 rpm overnight.

426 The cultivation for 1-undecene production from ferulate was carried out with ADP1 *'tesA-*
427 *undA* and adapted ADP1 *'tesA-undA*. Cells were precultivated in mineral salts medium
428 containing 5 mM ferulate and 25 µg/ml chloramphenicol at 30 °C and 300 rpm. The
429 chloramphenicol used in the cultivation was prepared with water to ensure that ferulate is
430 the only carbon source and energy source. ADP1 *'tesA-undA* was precultivated for 48 h
431 while adapted strain was precultivated for 24 h. After precultivation, cells were transferred
432 to 110 ml flasks supplemented with 12 ml mineral salts medium containing 110 mM
433 ferulate and 25 µg/ml chloramphenicol. The initial OD was 0.05. Cells were induced after

434 17 h of cultivation with 1 mM cyclohexanone. After 4.5 h of induction, 10 ml culture was
435 taken from each flask and evenly distributed to two sealed headspace 20 ml vials containing
436 stir bars (each vial contains 5 ml culture). The cells were then incubated at 25 °C and 300
437 rpm for 20 h.

438 **5.7 Analysis methods**

439 The consumption of carbon sources was analyzed with high performance liquid
440 chromatography (HPLC). The samples were collected from the cultures and centrifuged at
441 20000 g for 5 minutes. The supernatant was taken and filtered with syringe filters
442 (CHROMAFIL® PET, PET-45/25, Macherey-Nagel, Germany). The filtered supernatant
443 was diluted with sterile deionized pure water. The measurement of ferulate concentration
444 was performed with Agilent Technology 1100 Series HPLC (UV/VIS system) equipped
445 with G1313A auto sampler, G1322A degasser, G1311A pump and G1315A DAD. Rezex
446 RFQ-Fast Acid H⁺ (8%) (Phenomenex) was used as the column and placed at 80 °C.
447 Sulfuric acid (0.005 N) was used as the eluent with a pumping rate of 1 ml/minute.

448 The detection of 1-undecene was performed with SPME-GCMS described by Rui et al.
449 (2014). Briefly, after cultivation, the sealed headspace vials were placed in aluminum block
450 at 25 °C. At the same time, the culture was stirred with a magnetic stirrer. An SPME fiber
451 (d_f 30 µm, needle size 24 ga, polydimethylsioxane, Supelco, Sigma-Aldrich) was injected
452 into the vials and held for 12.5 minutes for absorption. GC-MS analysis was performed
453 with Agilent 6890N GC system with 5975B inert XL MSD. The analytes were desorbed
454 from the fiber in a splitless injector at 250 °C for 75 seconds and developed with helium as
455 carrier gas with a flow rate of 1 ml/min. Temperature gradient was applied: 50 °C for 3min,

456 temperature ramped to 130 °C with a rate of 10 °C/min, then ramped to 300°C with a rate
457 of 30 °C/min, 300 °C for 5 min.

458 **6 Acknowledgements**

459 The research work was supported by Academy of Finland (grants no. 286450, 310135,
460 310188, and 311986)

461 **7 References**

462 Abdelaziz, O.Y., Brink, D.P., Prothmann, J., Ravi, K., Sun, M., García-Hidalgo, J., Sandahl,
463 M., Hulteberg, C.P., Turner, C., Lidén, G., Gorwa-Grauslund, M.F., 2016. Biological
464 valorization of low molecular weight lignin. *Biotechnol. Adv.* 34, 1318–1346.
465 <https://doi.org/10.1016/j.biotechadv.2016.10.001>

466 Almario, M.P., Reyes, L.H., Kao, K.C., 2013. Evolutionary engineering of *Saccharomyces*
467 *cerevisiae* for enhanced tolerance to hydrolysates of lignocellulosic biomass.
468 *Biotechnol. Bioeng.* 110, 2616–2623. <https://doi.org/10.1002/bit.24938>

469 Atsumi, S., Wu, T.Y., MacHado, I.M.P., Huang, W.C., Chen, P.Y., Pellegrini, M., Liao,
470 J.C., 2010. Evolution, genomic analysis, and reconstruction of isobutanol tolerance in
471 *Escherichia coli*. *Mol. Syst. Biol.* 6, 1–11. <https://doi.org/10.1038/msb.2010.98>

472 Beckham, G.T., Johnson, C.W., Karp, E.M., Salvachúa, D., Vardon, D.R., 2016.
473 Opportunities and challenges in biological lignin valorization. *Curr. Opin. Biotechnol.*
474 42, 40–53. <https://doi.org/10.1016/j.copbio.2016.02.030>

475 Beller, H.R., Goh, E.B., Keasling, J.D., 2010. Genes involved in long-chain alkene

- 476 biosynthesis in *Micrococcus luteus*. *Appl. Environ. Microbiol.* 76, 1212–1223.
477 <https://doi.org/10.1128/AEM.02312-09>
- 478 Benedetti, I., Nikel, P.I., de Lorenzo, V., 2016. Data on the standardization of a
479 cyclohexanone-responsive expression system for Gram-negative bacteria. *Data Br.* 6,
480 738–744. <https://doi.org/10.1016/j.dib.2016.01.022>
- 481 Bleichrodt, F.S., Fischer, R., Gerischer, U.C., 2010. The β -ketoacid pathway of
482 *Acinetobacter baylyi* undergoes carbon catabolite repression, cross-regulation and
483 vertical regulation, and is affected by Crc. *Microbiology* 156, 1313–1322.
484 <https://doi.org/10.1099/mic.0.037424-0>
- 485 Calero, P., Jensen, S.I., Bojanovič, K., Lennen, R.M., Koza, A., Nielsen, A.T., 2018.
486 Genome-wide identification of tolerance mechanisms toward *p*-coumaric acid in
487 *Pseudomonas putida*. *Biotechnol. Bioeng.* 115, 762–774.
488 <https://doi.org/10.1002/bit.26495>
- 489 Cerisy, T., Souterre, T., Torres-Romero, I., Boutard, M., Dubois, I., Patrouix, J., Labadie,
490 K., Berrabah, W., Salanoubat, M., Doring, V., Tolonen, A.C., 2017. Evolution of a
491 biomass-fermenting bacterium to resist lignin phenolics. *Appl. Environ. Microbiol.* 83,
492 1–13. <https://doi.org/10.1128/AEM.00289-17>
- 493 Chen, B., Lee, D.Y., Chang, M.W., 2015. Combinatorial metabolic engineering of
494 *Saccharomyces cerevisiae* for terminal alkene production. *Metab. Eng.* 31, 53–61.
495 <https://doi.org/10.1016/j.ymben.2015.06.009>
- 496 Choi, Y.J., Lee, S.Y., 2013. Microbial production of short-chain alkanes. *Nature* 502, 571–

- 497 574. <https://doi.org/10.1038/nature12536>
- 498 De Menezes, F.F., Rencoret, J., Nakanishi, S.C., Nascimento, V.M., Silva, V.F.N.,
499 Gutiérrez, A., Del Río, J.C., De Moraes Rocha, G.J., 2017. alkaline pretreatment
500 severity leads to different lignin applications in sugar cane biorefineries. ACS Sustain.
501 Chem. Eng. 5, 5702–5712. <https://doi.org/10.1021/acssuschemeng.7b00265>
- 502 Dragosits, M., Mattanovich, D., 2013. Adaptive laboratory evolution -- principles and
503 applications for biotechnology. Microb Cell Fact 12, 64. [https://doi.org/10.1186/1475-](https://doi.org/10.1186/1475-2859-12-64)
504 2859-12-64
- 505 Fischer, R., Bleichrodt, F.S., Gerischer, U.C., 2008. Aromatic degradative pathways in
506 Acinetobacter baylyi underlie carbon catabolite repression. Microbiology 154, 3095–
507 3103. <https://doi.org/10.1099/mic.0.2008/016907-0>
- 508 Fitzgerald, D.J., Stratford, M., Gasson, M.J., Ueckert, J., Bos, A., Narbad, A., 2004. Mode
509 of antimicrobial of vanillin against Escherichia coli, Lactobacillus plantarum and
510 Listeria innocua. J. Appl. Microbiol. 97, 104–113. [https://doi.org/10.1111/j.1365-](https://doi.org/10.1111/j.1365-2672.2004.02275.x)
511 2672.2004.02275.x
- 512 Gerischer, U. (Ed.), 2008. Acinetobacter molecular biology. Horizon Scientific Press.
- 513 Hartmans, S., Smits, J.P., Van der Werf, M.J., Volkering, F., de Bont, J.A.M., 1989.
514 Metabolism of styrene oxide and 2-phenylethanol. Appl. Environ. Microbiol. 55,
515 2850–2855.
- 516 Harwood, C.S., Parales, R.E., 1996. The β -ketoadipate pathway and the biology of self-
517 identity. Annu. Rev. Microbiol. 50, 553–590.

- 518 <https://doi.org/10.1146/annurev.micro.50.1.553>
- 519 Ibraheem, O., Ndimba, B.K., 2013. Molecular adaptation mechanisms employed by
520 ethanogenic bacteria in response to lignocellulose-derived inhibitory compounds. *Int.*
521 *J. Biol. Sci.* 9, 598–612. <https://doi.org/10.7150/ijbs.6091>
- 522 Kang, M.K., Nielsen, J., 2017. Biobased production of alkanes and alkenes through
523 metabolic engineering of microorganisms. *J. Ind. Microbiol. Biotechnol.* 44, 613–622.
524 <https://doi.org/10.1007/s10295-016-1814-y>
- 525 Lee, J.-W., Niraula, N.P., Trinh, C.T., 2018. Harnessing a P450 fatty acid decarboxylase
526 from *Macrococcus caseolyticus* for microbial biosynthesis of odd chain terminal
527 alkenes. *Metab. Eng. Commun.* <https://doi.org/10.1016/j.mec.2018.e00076>
- 528 Lehtinen, T., Santala, V., Santala, S., 2017. Twin-layer biosensor for real-time monitoring
529 of alkane metabolism. *FEMS Microbiol. Lett.* 364, 1–7.
530 <https://doi.org/10.1093/femsle/fnx053>
- 531 Lehtinen, T., Virtanen, H., Santala, S., Santala, V., 2018. Production of alkanes from CO₂
532 by engineered bacteria. *Biotechnol. Biofuels* 11, 228. [https://doi.org/10.1186/s13068-](https://doi.org/10.1186/s13068-018-1229-2)
533 [018-1229-2](https://doi.org/10.1186/s13068-018-1229-2)
- 534 Linger, J.G., Vardon, D.R., Guarnieri, M.T., Karp, E.M., Hunsinger, G.B., Franden, M.A.,
535 Johnson, C.W., Chupka, G., Strathmann, T.J., Pienkos, P.T., Beckham, G.T., 2014.
536 Lignin valorization through integrated biological funneling and chemical catalysis.
537 *Proc. Natl. Acad. Sci.* <https://doi.org/10.1073/pnas.1410657111>
- 538 Liu, Q., Wu, K., Cheng, Y., Lu, L., Xiao, E., Zhang, Y., Deng, Z., Liu, T., 2015.

- 539 Engineering an iterative polyketide pathway in *Escherichia coli* results in single-form
540 alkene and alkane overproduction. *Metab. Eng.* 28, 82–90.
541 <https://doi.org/10.1016/j.ymben.2014.12.004>
- 542 Liu, Y., Wang, C., Yan, J., Zhang, W., Guan, W., Lu, X., Li, S., 2014. Hydrogen peroxide-
543 independent production of α -alkenes by OleTJE P450 fatty acid decarboxylase.
544 *Biotechnol. Biofuels* 7, 28. <https://doi.org/10.1186/1754-6834-7-28>
- 545 Metzgar, D., Bacher, J.M., Pezo, V., Reader, J., Döring, V., Schimmel, P., Marlière, P., de
546 Crécy-Lagard, V., 2004. *Acinetobacter* sp. ADP1: An ideal model organism for
547 genetic analysis and genome engineering. *Nucleic Acids Res.* 32, 5780–5790.
548 <https://doi.org/10.1093/nar/gkh881>
- 549 Mills, T.Y., Sandoval, N.R., Gill, R.T., 2009. Cellulosic hydrolysate toxicity and tolerance
550 mechanisms in *Escherichia coli*. *Biotechnol. Biofuels* 2, 1–11.
551 <https://doi.org/10.1186/1754-6834-2-26>
- 552 Peralta-Yahya, P.P., Zhang, F., Del Cardayre, S.B., Keasling, J.D., 2012. Microbial
553 engineering for the production of advanced biofuels. *Nature* 488, 320–328.
554 <https://doi.org/10.1038/nature11478>
- 555 Ragauskas, A.J., 2006. The path forward for biofuels and biomaterials. *Science* (80-.). 311,
556 484–489. <https://doi.org/10.1126/science.1114736>
- 557 Ragauskas, A.J., Beckham, G.T., Bidy, M.J., Chandra, R., Chen, F., Davis, M.F., Davison,
558 B.H., Dixon, R.A., Gilna, P., Keller, M., Langan, P., Naskar, A.K., Saddler, J.N.,
559 Tschaplinski, T.J., Tuskan, G.A., Wyman, C.E., 2014. Lignin valorization: improving

- 560 lignin processing in the biorefinery. *Science* (80-.). 344, 1246843–1246843.
561 <https://doi.org/10.1126/science.1246843>
- 562 Rinaldi, R., Jastrzebski, R., Clough, M.T., Ralph, J., Kennema, M., Bruijninx, P.C.A.,
563 Weckhuysen, B.M., 2016. Paving the way for lignin valorisation: recent advances in
564 bioengineering, biorefining and catalysis. *Angew. Chemie - Int. Ed.*
565 <https://doi.org/10.1002/anie.201510351>
- 566 Rui, Z., Harris, N.C., Zhu, X., Huang, W., Zhang, W., 2015. Discovery of a family of
567 desaturase-like enzymes for 1-alkene biosynthesis. *ACS Catal.* 5, 7091–7094.
568 <https://doi.org/10.1021/acscatal.5b01842>
- 569 Rui, Z., Li, X., Zhu, X., Liu, J., Domigan, B., Barr, I., Cate, J.H.D., Zhang, W., 2014.
570 Microbial biosynthesis of medium-chain 1-alkenes by a nonheme iron oxidase. *Proc.*
571 *Natl. Acad. Sci.* 111, 18237–18242. <https://doi.org/10.1073/pnas.1419701112>
- 572 Salmela, M., Sanmark, H., Efimova, E., Efimov, A., Hytönen, V.P., Lamminmäki, U.,
573 Santala, S., Santala, V., 2018. Molecular tools for selective recovery and detection of
574 lignin-derived molecules. *Green Chem.* <https://doi.org/10.1039/c8gc00490k>
- 575 Salvachúa, D., Karp, E.M., Nimlos, C.T., Vardon, D.R., Beckham, G.T., 2015. Towards
576 lignin consolidated bioprocessing: simultaneous lignin depolymerization and product
577 generation by bacteria. *Green Chem.* <https://doi.org/10.1039/C5GC01165E>
- 578 Santala, S., Efimova, E., Kivinen, V., Larjo, A., Aho, T., Karp, M., Santala, V., 2011.
579 Improved triacylglycerol production in *Acinetobacter baylyi* ADP1 by metabolic
580 engineering. *Microb. Cell Fact.* 10, 1–10. <https://doi.org/10.1186/1475-2859-10-36>

- 581 Santala, S., Efimova, E., Koskinen, P., Karp, M.T., Santala, V., 2014a. Rewiring the wax
582 ester production pathway of acinetobacter baylyi ADP1. ACS Synth. Biol. 3, 145–151.
583 <https://doi.org/10.1021/sb4000788>
- 584 Santala, S., Karp, M., Santala, V., 2014b. rationally engineered synthetic coculture for
585 improved biomass and product formation. PLoS One 9, e113786.
586 <https://doi.org/10.1371/journal.pone.0113786>
- 587 Sarria, S., Kruyer, N.S., Peralta-Yahya, P., 2017. Microbial synthesis of medium-chain
588 chemicals from renewables. Nat. Biotechnol. 35, 1158–1166.
589 <https://doi.org/10.1038/nbt.4022>
- 590 Schirmer, A., Rude, M.A., Li, X., Popova, E., del Cardayre, S.B., 2010. Microbial
591 biosynthesis of alkanes. Science (80-.). 329, 559–562.
592 <https://doi.org/10.1126/science.1187936>
- 593 Steen, E.J., Kang, Y., Bokinsky, G., Hu, Z., Schirmer, A., McClure, A., Del Cardayre, S.B.,
594 Keasling, J.D., 2010. Microbial production of fatty-acid-derived fuels and chemicals
595 from plant biomass. Nature 463, 559–562. <https://doi.org/10.1038/nature08721>
- 596 Steigedal, M., Valla, S., 2008. The Acinetobacter sp. chnB promoter together with its
597 cognate positive regulator ChnR is an attractive new candidate for metabolic
598 engineering applications in bacteria. Metab. Eng. 10, 121–129.
599 <https://doi.org/10.1016/j.ymben.2007.08.002>
- 600 Vardon, D.R., Franden, M.A., Johnson, C.W., Karp, E.M., Guarnieri, M.T., Linger, J.G.,
601 Salm, M.J., Strathmann, T.J., Beckham, G.T., 2015. Adipic acid production from

- 602 lignin. *Energy Environ. Sci.* 8, 617–628. <https://doi.org/10.1039/C4EE03230F>
- 603 Zhao, Z., Moghadasian, M.H., 2008. Chemistry, natural sources, dietary intake and
604 pharmacokinetic properties of ferulic acid: A review. *Food Chem.* 109, 691–702.
605 <https://doi.org/10.1016/j.foodchem.2008.02.039>
- 606 Zheng, Y., Li, L., Liu, Q., Yang, J., Cao, Y., Jiang, X., Zhao, G., Xian, M., 2012. Boosting
607 the free fatty acid synthesis of *Escherichia coli* by expression of a cytosolic
608 *Acinetobacter baylyi* thioesterase. *Biotechnol. Biofuels* 5, 76.
609 <https://doi.org/10.1186/1754-6834-5-76>
- 610 Zhou, Y.J., Kerkhoven, E.J., Nielsen, J., 2018. Barriers and opportunities in bio-based
611 production of hydrocarbons. *Nat. Energy*. <https://doi.org/10.1038/s41560-018-0197-x>

612 **8 Figure captions**

613 Figure 1. A schematic representation of the medium-chain alkene production from LDMs
614 by *A. baylyi* ADP1. Various LDMs can be converted into central metabolites by *A. baylyi*
615 ADP1. Genes '*tesA* and *undA*, encoding for thioesterase and decarboxylase, respectively,
616 are heterologously expressed in *A. baylyi* ADP1 for alkene production. 1-Undecene is a
617 semivolatile hydrocarbon, which can be directly collected from the culture headspace.

618 Figure 2. The growth of adapted ADP1 (A) and wild-type ADP1 (B) on ferulate. The
619 strains were cultured in mineral salts medium supplemented with 15 mM, 30 mM, 45 mM,
620 60 mM, 80 mM, and 100 mM ferulate. The mean values and standard deviations (error bars)
621 from three parallel cultures are shown.

622 Figure 3. Production of 1-undecene from glucose by *A. baylyi* ADP1 with different
623 constructs. In the histogram, from the left to the right are 1-undecene productions with
624 ADP1- empty plasmid pBAV1C- chn (control), ADP1 *UndA*, ADP1 '*tesA*', and ADP1
625 '*tesA-undA*'. The mean values and standard deviations (error bars) from two parallel
626 cultures are shown.

627 Figure 4. Growth and 1-undecene production by ADP1 '*tesA-undA*' and adapted ADP1
628 '*tesA-undA*' from ferulate. (A) The biomasses (OD) and ferulate concentrations of adapted
629 ADP1 '*tesA-undA*' and ADP1 '*tesA-undA*'. The strains were cultivated in mineral salts
630 medium supplemented with 110 mM ferulate. The cells were induced after 17 h of
631 incubation in aerated flasks, and thereafter incubated in sealed vials for 20 hours. The
632 values of the last sampling point are the mean from two parallel cultures and the error bars
633 represent the standard deviations (the standard deviations are low, and thus the error bars
634 are not visible in the figure). (B) 1-Undecene production from ferulate as the sole carbon
635 source. 1-undecene was directly collected from the culture headspace. The mean values and
636 standard deviations (error bars) from two parallel cultures are shown.

637

638

639

640

641

642 9 Tables and Figures

643 Table 1 List of primers used in this study

Name	Description	Oligo sequence (5-3')
ab156	chnR/pChnB, PstI	GTTTCTTCTGCAGCGCCGCTACTAGTAGATTACGACATGTGAATTTATTCAAATC TGC
ab155	chnR/pChnB, EcoRI	GTTTCTTCGAATTCGCGGCCGCTTCTAGAGTCTAGGGCGGCGGATTTGTCC
ab152	pBAVIC rev.	TCATGAATCAAAGGACGCTATTG
ab151	pBAVIC for.	GTCAAATATTCATAAGAACCCTTTGATATAATC
GFP fwd	GFP	TGGAATTCGCGGCCGCTTCTAGAGAAAGAGGAGAAATACTAGATGCGTAAAGGTGA AGAACTGTTTAC
GFP rev	GFP	TAATACTGCAGTTAAGCTACTAAAGCGTAGTTTTTCGTCGTTTGCAGCAGGCCTTTTGT AGAGTTCATCCATGCCGTG
vs15_2 44	<i>undA</i> , PstI	TAATCTGCAGCGGCCGCTACTAGTATTATCAGCCCGCAGCCAAC
vs15_1 68	<i>undA</i> , XbaI	TAATGAATTCGCGGCCGCTTCTAGAGAAAGAGGAGAAATACTAGATGATTGACGCA TTTGTTCGTATC
tl15	<i>'tesA</i> , XbaI	TGGAATTCGCGGCCGCTTCTAGAGAAAGAGGAGAAATACTAGATGGCGGACACGTT ATTGATTCTGGG
tl16	<i>'tesA</i> , PstI	GTTTCTTCTGCAGCGGCCGCTACTAGTATTATTATGAGTCATGATTTACTAAAGGCT GC

644

645

646

647

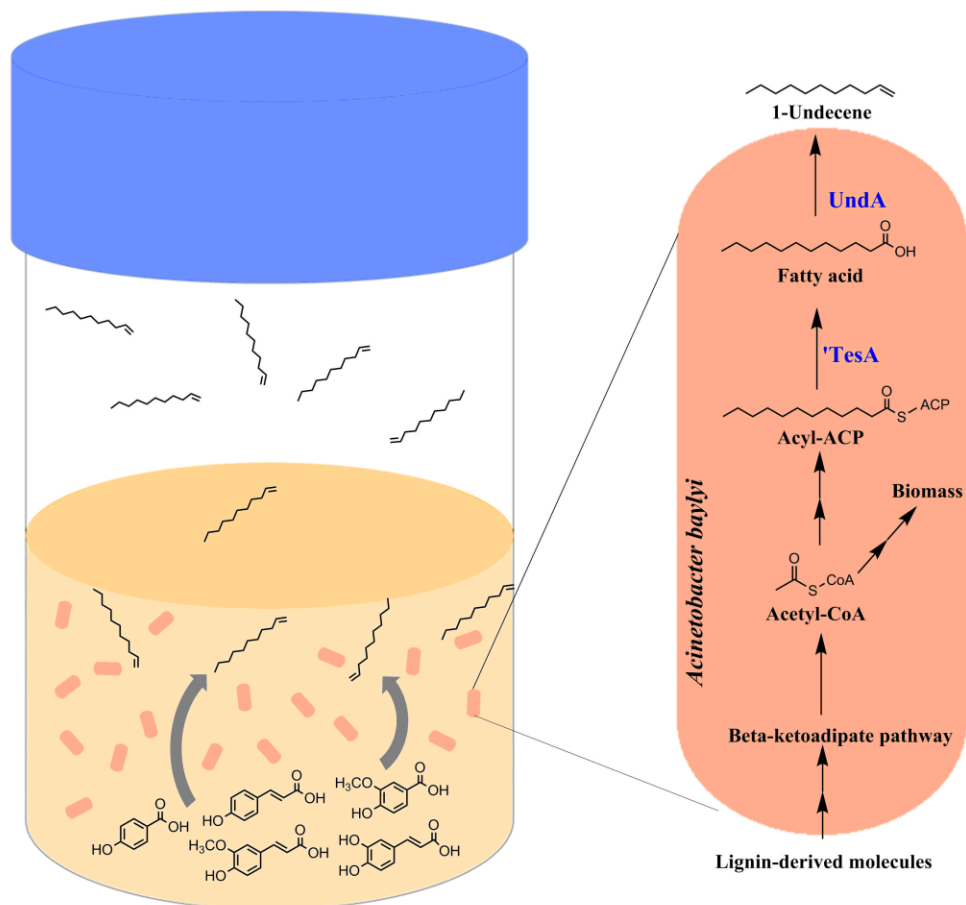
648

649

650

651

652 **Figure 1**



653

654

655

656

657

658

659

660

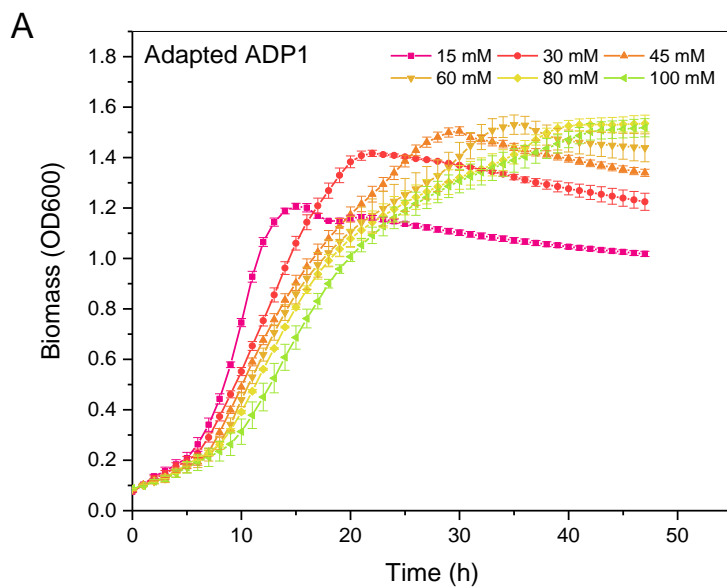
661

662

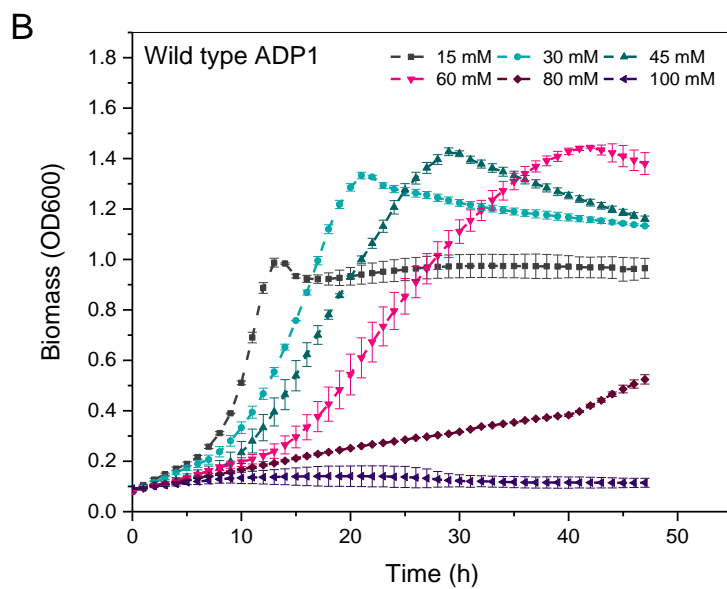
663

664

665 **Figure 2**



666

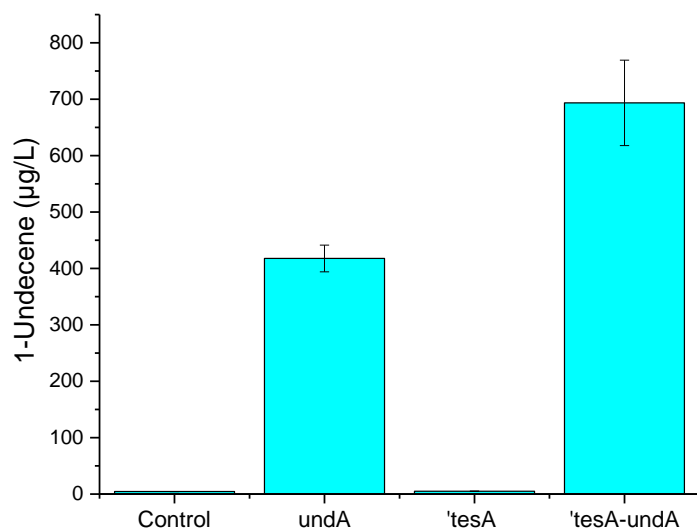


667

668

669

670 **Figure 3**



671

672

673

674

675

676

677

678

679

680

681

682

683

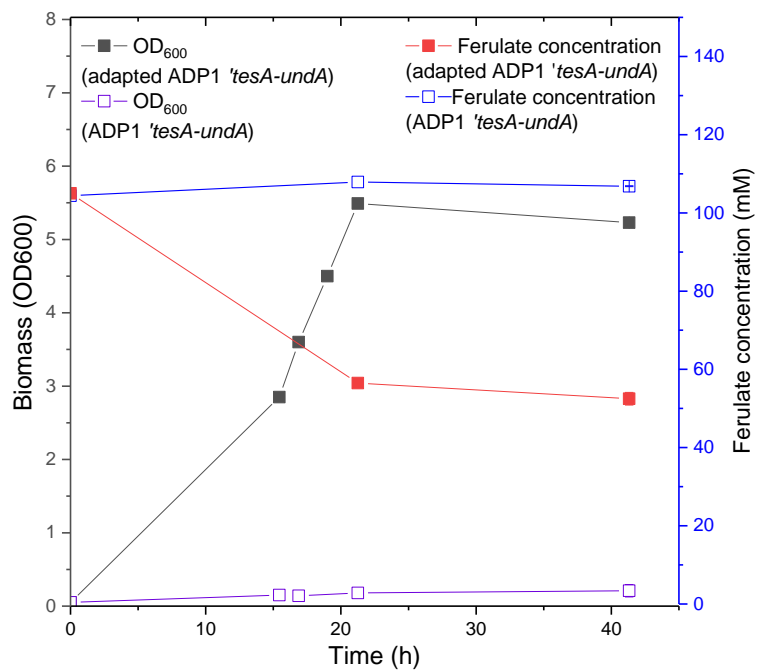
684

685

686

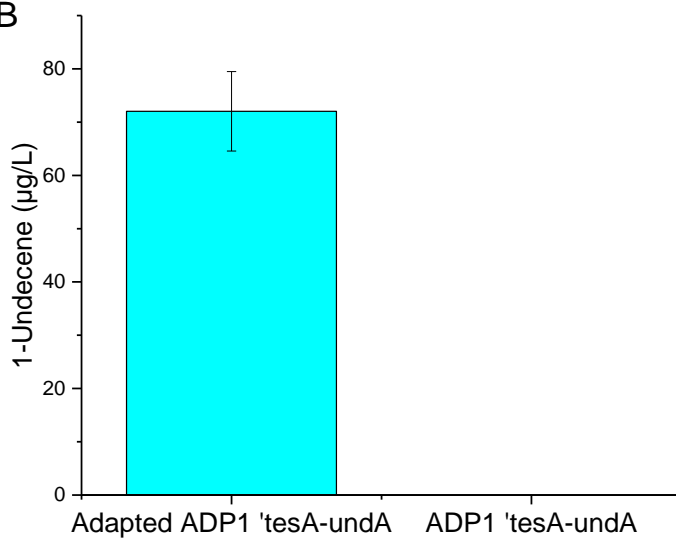
687 **Figure 4**

A



688

B



689